Available online at www.sciencedirect.com
SCIENCE DIRECT®
International Journal of Heat and Mass Transfer 48 (2005) 2032–2041
International Journal of HEAT and MASS TRANSFER
www.elsevier.com/locate/ijhmt

Observations of high temperature impinging-jet boiling phenomena

Peter Lloyd Woodfield [a,*], Masanori Monde [a,1], Aloke Kumar Mozumder [b,2]

[a] Institute of Ocean Energy, Saga University, 1 Honjo-machi, Saga 840-8502, Japan
[b] Department of Mechanical Engineering, Saga University, 1 Honjo-machi, Saga 840-8502, Japan

Received 23 July 2004
Available online 26 February 2005

Abstract

A high-speed video camera and microphone were used to capture the flow behavior and boiling sound of a free-surface water jet impinging on a high temperature surface during quench cooling. It was found that depending on the superheat of the surface considerably different flow patterns appeared. For cases where the initial surface temperature was above about 300 °C an almost explosive pattern appeared. This was in contrast to slightly lower temperatures where a liquid sheet flow structure was apparent. The change in phenomena was accompanied by a sudden change in the boiling sound and an increase in the heat transfer rate.

Keywords: Transition boiling; Flow phenomena; Quench; Jet impingement

1. Introduction

In the boiling literature it is common to relate and interpret observed phenomena for different flow situations in the light of classical results from pool boiling experiments. While this approach provides a very useful structure for understanding boiling, due to the complex nature and diversity of situations in which boiling occurs we cannot expect that every case will fit the mold exactly. For quench cooling of a high temperature solid using an impinging jet, a unique set of circumstances arises that has been found to not always produce a one-to-one correspondence with the pool boiling data. The basic boiling modes: nucleate boiling, transition boiling and film boiling occur and usually can be identified for impinging jets [1]. However, the boundaries of the regimes are typically shifted to significantly greater superheats, moving the boiling modes that involve direct liquid/solid contact closer to the critical temperature for the fluid. Significantly higher heat fluxes occur and during the quench, the system experiences different boiling modes at different times and sometimes simultaneously at different spatial positions. Due to the complexity and transient nature of the problem, the flow behavior and mechanism for phase change during quenching from high temperatures is not well defined at present.

A number of unusual phenomena have been reported for quench cooling by impinging jets. Ishigai et al. [2]

* Corresponding author. Tel.: +81 952 26 3870; fax: +81 952 28 8595.
E-mail addresses: peter@me.saga-u.ac.jp (P.L. Woodfield), monde@me.saga-u.ac.jp (M. Monde), 03ts11@edu.cc.saga-u.ac.jp (A.K. Mozumder).
[1] Tel.: +81 952 28 8608; fax: +81 952 28 8587.
[2] Tel.: +81 952 28 3216; fax: +81 952 28 8595.

0017-9310/$ - see front matter © 2005 Elsevier Ltd. All rights reserved.
doi:10.1016/j.ijheatmasstransfer.2004.12.011

Nomenclature

a	thermal diffusivity
C	constant defined by Eq. (4)
C_0	coefficient for eigen function ($j = 0$)
C_j	coefficient for eigen function
c_p	specific heat capacity of liquid
d	diameter of jet
D	diameter of apparent liquid/solid contact region
F_1	function defined by Eq. (A.6d)
F_2	function defined by Eq. (A.6e)
F_3	function defined by Eq. (A.6f)
F_4	function defined by Eq. (A.6g)
G	analytical solution for temperature change with constant heat flux boundary condition
H	height of the cylinder
h_{fg}	latent heat of vaporization
Ja	Jacob number
k	index for summation
m_j	eigen value
q	heat flux
q_0	heat flux beneath jet for $0 < t < t^*$
q_0^*	heat flux beneath jet for $t > t^*$
q_1	heat flux for $r > r_0$
r	radial position
r_0	radial position for step change in heat flux
R	radius of cylinder
t	Time
t^*	time at which heat flux changes
T	temperature
T_0	initial temperature of solid
T_{liq}	liquid temperature
u_j	jet velocity
z	axial position

Greek symbols

ΔT_{sub}	liquid subcooling
ΔT_{sat}	solid superheat
λ	thermal conductivity
ρ	density
σ	surface tension

Subscripts

j	corresponding to the jth eigen value
l	liquid
v	vapor
c	critical heat flux
co	critical heat flux for saturation temperature

performed experiments with a planar, subcooled, free-surface water jet impinging on a surface with an initial temperature of approximately 1000 °C. They found that a region of almost constant heat flux appeared in the transition regime for liquid subcoolings greater than $\Delta T_{sub} = 15$ K. This 'shoulder' in the transition regime also was reported by Auracher and Marquardt [3] and Robidou et al. [4] in steady-state experiments. Their data showed that the effect occurred in the stagnation region of a 1×9 mm planar water jet for a jet velocity of 0.8 m/s and a subcooling of 16 K at atmospheric pressure. In the parallel flow region of the jet, the shoulder did not appear in the boiling curve. In addition, for the stagnation zone their boiling curves showed two minimum heat flux points. One was at a superheat of about $\Delta T_{sat} = 90$ K and the other at a superheat of $\Delta T_{sat} = 360$ K. This is a radical departure from the classical boiling curve.

Hammad and Monde [5,6] investigated the movement of the wetting front during quench cooling of a 94 mm diameter high temperature cylindrical block using an impinging jet. They simultaneously recorded the temperature distribution in the solid and the position of the wetting front with a high-speed video camera. Using a two-dimensional inverse heat transfer solution [7], they calculated the instantaneous temperature distribution and heat flux based on the temperatures measured within the solid. They found that for high temperatures there was a significant delay before movement of the wetting front across the hot surface. For a copper test piece, in some cases the delay lasted for about 30 min and then suddenly the liquid front moved across the surface. The delay was found to increase for lower jet velocities and higher liquid temperatures.

Piggott et al. [8] also reported a delay to the movement of the wetting front. In addition, they observed a number of completely different flow patterns during quenching of 6.3–25.3 mm diameter heated rods from an initial temperature of 700 °C with a subcooled water jet. During their experiment a constant power supply to the heater was maintained. The most dramatic phenomena occurred for the case where the outermost layer of the heated rod was a 1 mm thick gold tube. The quench began with quiet film boiling and then a white patch around 5 mm in diameter appeared beneath the jet. The liquid film then broke into tiny droplets in a spray pattern, which was followed by an oscillating liquid sheet that lifted from the surface of the rod. Finally the wetting front moved forward over the heated surface.

Liu and Wang [9] carried out an experimental investigation to measure heat transfer to an impinging jet during film boiling on a high temperature plate. They

reported a significant increase in the heat flux with liquid subcooling and heat fluxes in the range from 0.2 to 2 MW/m^2 for film boiling. These figures are over an order of magnitude greater than film boiling at the minimum heat flux condition for pool boiling which reflects the heat transfer enhancement of impinging jets. The solid superheats reported for the minimum heat flux condition in their experiments were as high as $\Delta T_{sat} = 700$ K for a liquid subcooling of $\Delta T_{sub} = 45$ K, which is a similar order of magnitude of those determined by Ishigai et al. [2]. Hall et al. [10] pointed out that if the reported surface superheat is accurate in the experiments by Ishigai et al. then the minimum heat flux condition for these special circumstances cannot correspond to a re-wetting phenomenon since the fluid temperature at the interface will be greater than the critical temperature for water.

Hatta et al. [11] considered quench cooling of a 10 mm thick stainless steel plate from an initial temperature of around 900 °C using a subcooled laminar water jet ($\Delta T_{sub} = 80$ K). Visual observations indicated an almost instantaneous drop in surface temperature to below 500 °C since the metal color in a small circle beneath the jet changed from glowing red to black immediately when the jet contacted the surface. From this they concluded that direct liquid solid contact occurred without any noticeable period of film boiling in spite of the high temperature.

Presently our understanding of the nature of the phase change phenomena and characteristics of heat transfer for impinging jets in the high temperature context is limited. A comprehensive review of jet impingement boiling was made by Wolf et al. [1]. They observed that in contrast to research on nucleate boiling and critical heat flux, there is a scarcity of concrete studies relating to jet impingement for the film boiling and transition regimes. They also pointed out that the most significant factor limiting theoretical studies for film and transition boiling is the uncertainty in the surface boundary condition. Further research in this field is of great practical value since, for example, in the metallurgical industry, for steel products the initial temperature for quench cooling is typically around 800 °C and 400–500 °C for light aluminum alloys [12].

The purpose of the present article is to report on some observed flow phenomena, which occurred in a jet impingement quench cooling experiment for solid temperatures in the vicinity of the homogeneous nucleation temperature for the liquid.

2. Experiment

Fig. 1 shows the basic setup for the quench cooling experiment. The key components of the apparatus were

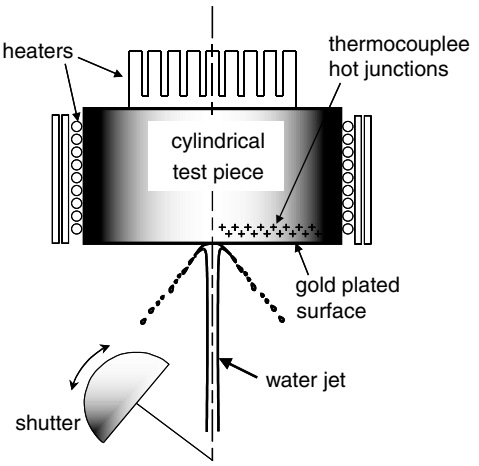

Fig. 1. Schematic of experimental test section.

a heated cylindrical test piece, a water jet, a number of electrical heaters and a spring-loaded shutter. The cylindrical test piece was copper or brass and had a diameter of 94 mm and a height 59 mm. The test surface was polished and plated with a 16 μm layer of gold to reduce oxidation effects. The surface roughness was 0.2–0.4 μm. The liquid jet issued from a nozzle 2 mm in diameter located 45 mm from the test surface. Three electrical heaters were used to heat the solid having a combined power of about 2.1 kW.

Sixteen thermocouples were embedded within the solid to record the thermal history as the block cooled. The thermocouples were high quality chromel/alumel type with the hot junction enclosed in a 1 mm diameter sheath. The thermocouple response time was experimentally verified to be around 0.1 s. Eight of the thermocouples were located at a depth 2.1 mm from the surface and the other 8 were 5 mm from the surface. The closest thermocouple to the center of the test surface was at a radial location of 4 mm from the center and a depth of 5 mm. The hot junctions were inserted in holes that were drilled parallel to the test surface and perpendicular to the radial line of measurement [6]. This minimized the depth positioning error and the symmetry of the flow pattern demonstrated that the effect of holes on the quench behavior was small. The thermocouples were connected to a multi-channel amplifier and then to a personal computer to store the readings during the quench. Readings were taken at a frequency of 20 per second, which was more than adequate for the present purpose and still slow compared with the 8 ms required by the AD card to scan all 16 channels.

The entire experimental test section shown in Fig. 1 was enclosed in a nitrogen atmosphere as an additional measure to reduce oxidation. However, in order to take clear photographs it was necessary to open the door allowing some oxygen to enter the system.

The experimental procedure was to first fill the liquid tank with around 20 L of distilled water. The test surface then was wiped and cleaned with acetone. The block and the water were heated to the desired initial temperatures while continuously pumping the water though a closed loop cycle with the shutter closed. When the thermocouples indicated that solid had reached the required temperature, the heaters were switched off. Due to rapid heating, there was a small temperature gradient in the solid, which caused the temperature near the surface to continue to rise a few °C above the intended initial condition after the power to the heaters was disconnected. During the next 3 or 4 min the temperature gradients in the solid evened out and the solid began to cool slowly and uniformly at about 0.1 K/s. When it had cooled to the desired initial condition, the shutter shown in Fig. 1 was opened allowing the jet to strike the surface. At the same time a high-speed video camera was employed to capture the flow pattern and a microphone to record the sound after impact.

3. Results

3.1. Video images of phenomenon

Fig. 2 shows the flow behavior for eight different initial temperatures. The images are for 4 ms after the jet impacted with the surface. The base material was copper; the liquid temperature was 80 °C and the jet velocity, 3 m/s. For reference purposes, Fig. 2(a) shows the flow pattern for an initial solid temperature of 104 °C. For the given surface, the superheat of 4 K was not enough for the onset of nucleation boiling so the effect shown is purely that of hydrodynamics. The radial position of the liquid front in Fig. 2(a) is about 10.5 mm from the center suggesting an average speed of the liquid of 2.6 m/s. Thus the average velocity of the fluid decreased only about 10% during the first 10 mm.

Fig. 2(b) gives the result for an initial temperature of 150 °C. In this case the effects of boiling are clearly evident. The liquid film is lifted from the surface and breaks into droplets. Fig. 2(c) and (d) is more chaotic than Fig. 2(b) suggesting a stronger influence of nucleation boiling on the flow pattern as the superheat increased. In contrast with Fig. 2(c) and (d), Fig. 2(e) and (f) shows a surprisingly calm and regular flow pattern. For these cases the initial solid temperature was 261 °C and 300 °C. The flow pattern for Fig. 2(e) and (f) can be described as a shallow conical sheet of liquid that finally breaks into droplets around 8 mm from the center. The dark shadow about 5 mm from the center in Fig. 2(f) suggests some boiling activity is occurring although it is not sufficiently vigorous to rupture the liquid sheet. For higher initial solid temperatures 325 °C and 378 °C, the flow pattern changes again. In Fig. 2(g) and (h), the jet is disintegrated into thousands of tiny droplets in an almost explosive pattern. This is completely different to the result shown in Fig. 2(e) and (f).

The results shown in Fig. 2 are for different experiments beginning at different initial temperatures. Similar flow patterns to those shown in Fig. 2 could be observed as the solid cooled in a single experiment beginning from 350 °C. The clearest photographs could be taken during the first few milliseconds of the quench because the presence of many liquid droplets obstructed the view of the camera at later times.

For a brass test piece with the same jet velocity and subcooling as shown for copper in Fig. 2, the same explosive pattern, Fig. 2(g) and (h), could not be observed even for initial solid temperatures as high as 400 °C. However, a liquid sheet pattern similar to Fig. 2(f) did appear for temperatures below 300 °C. Moreover, the flow structure oscillated back and forth between two patterns over a period of about 10 s during the quench. Fig. 3 shows the two patterns observed in the case of a brass test piece during quenching from an initial temperature of 300 °C. The flow pattern in Fig. 3(a) is for a time of 4.001 s after the jet struck the surface. The same pattern, as in Fig. 3(a), was observed whenever the sheet disappeared and also continuously for solid temperatures well above 300 °C in other experiments. In some cases the droplets were seen to depart from the surface in regular rings with a frequency of around 1000 rings per second.

Fig. 3(b) shows the typical sheet pattern observed during the quench for brass. The sheet structure in Fig. 3(b) has a radius of 12–15 mm, which is larger than the case for copper shown in Fig. 2(f). Another interesting feature is the angle at which droplets depart from the surface. It has been noted by other researchers that this angle changes during the quench [10,14]. From Fig. 3 it is clear that the angle between the hot surface and the path of the droplets is significantly greater when the sheet is present than when it is absent.

Fig. 4 illustrates how the flow structure swapped back and forth between the two cases shown in Fig. 3 during the first 12 s of the quench. Immediately after the jet struck the surface there was a period of about 1.2 s where there was no sheet pattern. This was followed by the appearance and then disappearance of the sheet. The period of time when the sheet was present gradually became longer until the sheet remained continuously after about 11 s. Piggott et al. [8] reported a similar oscillating liquid sheet phenomenon during jet-impingement quenching of an 18 mm diameter heated rod. In their case the liquid sheet remained intact during the oscillation with dramatic changes in the angle between the sheet and the hot surface.

Table 1 summarizes the statistics for the case shown in Fig. 4. The shortest period with the sheet was 4 ms

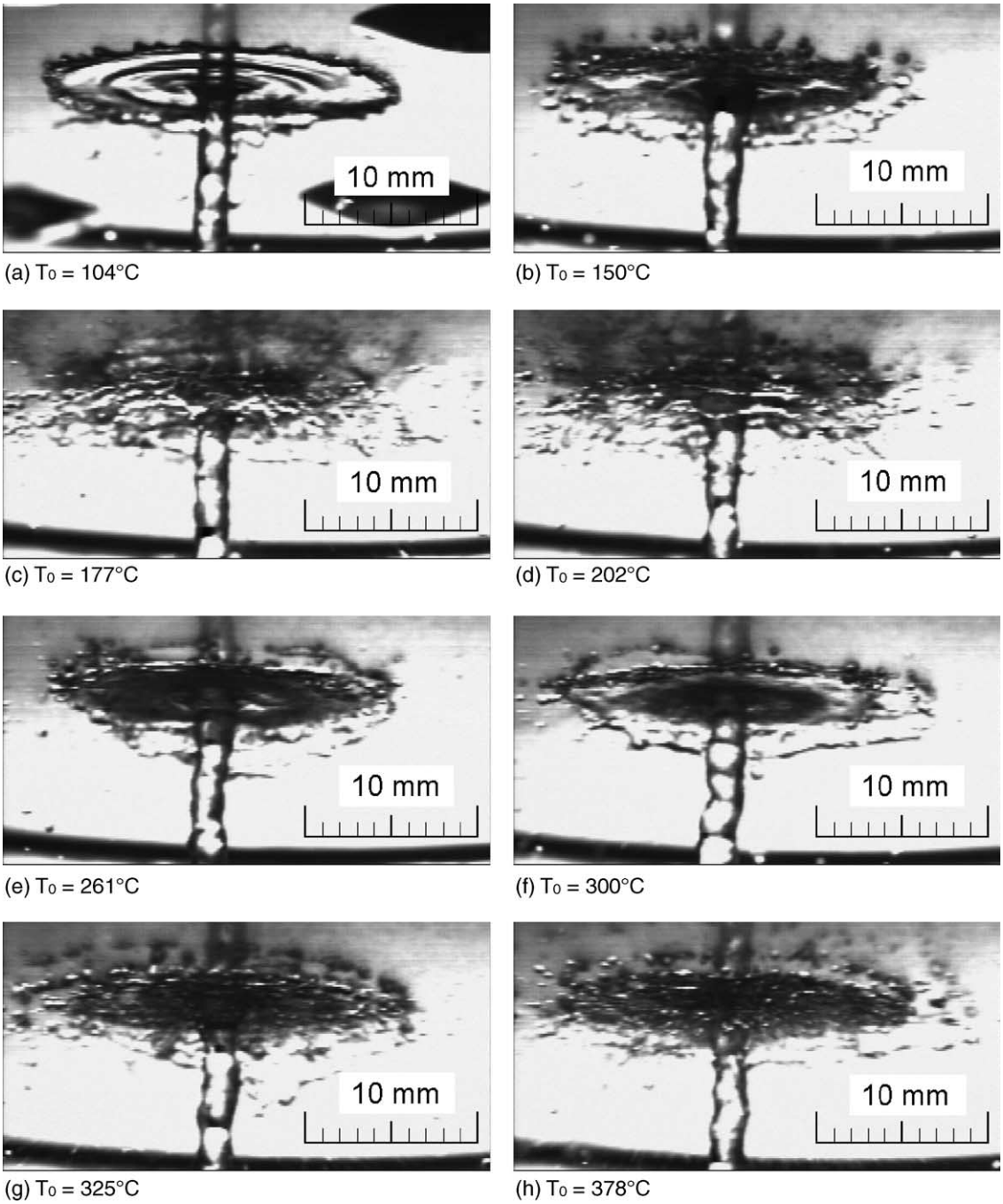

Fig. 2. Video images taken 4 ms after the jet struck the surface (copper, T_{liq} = 80 °C, u_j = 3 m/s).

and without the sheet was 22 ms. The maximum cycle took a little over one second and the average frequency of the cycle was 2.88 Hz. These time scales are large compared with the ratio d_{jet}/v_{jet} = 0.67 ms which is greater than the largest possible turbulence time scale. Thus it appears reasonable to conclude that the oscillating phenomenon shown in Fig. 4 and Table 1 is the result of longer thermal time lags on the solid side arising from changes in the heat flux and boiling conditions for which the sheet flow structure can appear.

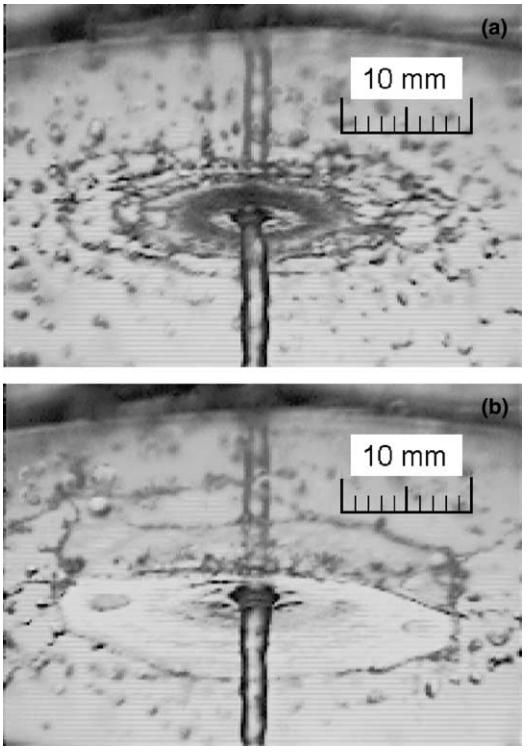

Fig. 3. Two flow patterns observed during quench of the brass test piece from 300 °C: (a) no sheet (t = 4.001 s) and (b) with sheet (t = 4.047 s).

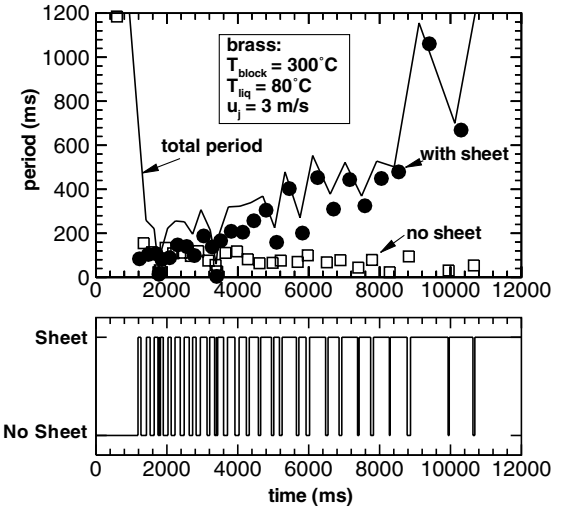

Fig. 4. Oscillation between two flow patterns for brass (T_0 = 300 °C, T_{liq} = 80 °C, u_j = 3 m/s).

3.2. Audible sounds during quench

As already indicated, during the quench a number of changes could be observed both visually and audibly.

Table 1
Statistics for Fig. 4 (in time period from 1.185 s to 10.687 s)

	With sheet	No sheet	Cycle
Minimum period	4 ms	22 ms	36 ms
Maximum period	1061 ms	155 ms	1156 ms
Average period	267 ms	80 ms	347 ms
Average frequency	–	–	2.88 Hz

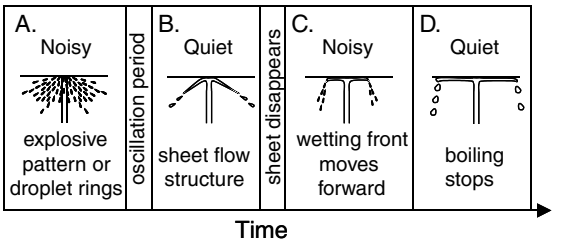

Fig. 5. Phenomenological history during quench.

Fig. 5 summarizes how the phenomena changed. Initially there was a noisy period where the flow pattern had the appearance of either Fig. 2(h) or Fig. 3(a). Following this the flow pattern changed to that shown in Fig. 3(b) and in some cases near the change over point there was an oscillating behavior between the two flow patterns as was illustrated in Fig. 4. During the time that the sheet structure was present the boiling sound became very quiet (Fig. 5B). After this the sheet disappeared and the wetting front moved forward over the surface. For this period the splattering boiling sound was again apparent (Fig. 5C). Finally as the surface of the test piece cooled to near the saturation point the boiling stopped and experiment became quiet (Fig. 5D).

The four regimes described in Fig. 5 are clearly demonstrated in Fig. 6, which shows the signal from the microphone during the quench. This case is for a copper test piece, a jet velocity of 3 m/s and a liquid temperature of 49 °C. During the first 120 s in Fig. 6, a sharp splattering sound could be heard, which corresponds to region A in Fig. 5. During the next 100 s the sheet flow pattern was present and the amplitude of the sound signal is small (region B). The wetting front began to move at around 200 s (region C) and finally convection heat transfer dominated by 300 s (region D).

Also included in Fig. 6 is the cooling history recorded by a thermocouple located 4 mm from the center and 5 mm from the surface of the block. It is interesting to note that the sudden change in the recorded sound and flow phenomena occurred when the metal temperature was around 280 °C, which is of the order of the homogeneous nucleation temperature for water at one atmospheric pressure [13].

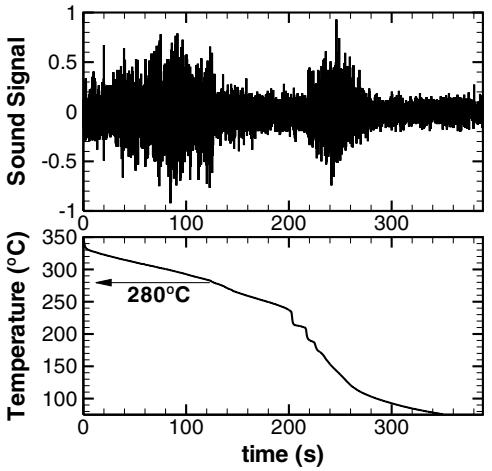

Fig. 6. Audible sound during quench (embedded thermocouple reading: 4 mm from center, 5 mm from surface, copper, $u_j = 3$ m/s $T_{liq} = 49$ °C).

3.3. Cooling curves and heat transfer rate

It is also apparent in Fig. 6 that there is a change in slope of the cooling curve after the point where the sound changed. In some cases the change in slope is more distinct as is for the case shown in Fig. 7. To obtain an approximate estimate of the heat flux before and after the change from region A to region B in Fig. 5, a two-dimensional analytical solution for the cylinder was employed (see Appendix A). It was assumed that the boundary heat flux profile was a 'top-hat' shape, which remained constant during region A and then a step change in the profile occurred at the time when the phenomenon changed. In an iterative procedure, the magnitudes of the heat flux in the center of the top-hat profile before and after the change were chosen so that predicted temperatures within the solid best matched the temperatures measured by the thermocouples. The accuracy of this kind of approach to the inverse heat conduction problem depends on how well the assumed profile shape approximates the actual heat flux distribution. In the present case, the chosen profile has some justification since good agreement between thermocouple readings and the analytical solution could be obtained.

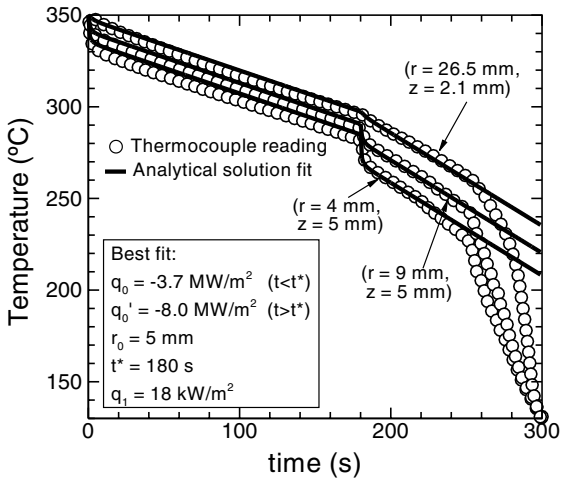

Fig. 7. Cooling curves during quench for copper block $T_0 = 350$ °C, $T_{liq} = 51$ °C, $u_j = 3$ m/s.

The smaller radius of the top-hat profile, r_0, was taken to be 5 mm, which corresponds to the apparent radius of the contact region for the jet from visual observations. The heat flux in the brim section of the top-hat profile, q_1, was taken to be 18 kW/m^2, to account for losses due to radiation and conduction of heat into the experimental apparatus through the supports for the block. This value was chosen since it gave the experimentally determined cooling rate of the block under ambient conditions while the jet was switched off.

Fig. 7 compares the thermocouple readings with temperatures estimated using the analytical solution assuming that the heat flux beneath the jet based on a radius of 5 mm was 3.7 MW/m^2 before the change in phenomenon and then 8.0 MW/m^2 after 180 s. The agreement with the measured results is quite good up until the wetting front began to move forward at around 250 s. This indicates that the simplified model analytical solution is a reasonable approximation to the actual situation within the time and space resolutions that can be detected using the present experimental apparatus. Thus we may conclude that for the given conditions in Fig. 7, the heat flux for the sheet flow pattern was about double that of the flow pattern without the sheet based on a radius of 5 mm.

It should be noted that in the center region the above heat flux estimate is an average in both time and space due to the thermal inertia of the solid. High frequency modes are rapidly smoothed with depth from the surface and thus the thermocouples are unable to detect the rapid fluctuations in the temperature of the surface, which occur during transition boiling. The value of 8.0 MW/m^2 for the sheet flow pattern is an averaged value which may correspond to the shoulder in the boiling curve reported by Ishigai et al. [2] for superheats higher than the critical heat flux point.

It is interesting to compare the experimentally determined heat fluxes with an estimate for the critical heat flux. Eq. (1) shows a well-known relation developed by Monde [15] for critical heat flux of a jet at the liquid saturation temperature.

$$\frac{q_{co}}{\rho_v h_{fg} u_j} = 0.221 \left(\frac{\rho_l}{\rho_v}\right)^{0.645} \left(\frac{2\sigma}{\rho_l u_j^2 (D-d)}\right)^{0.343} (1 + D/d)^{-0.364} \quad (1)$$

The effect of liquid subcooling is accounted for using the following relation.

$$\frac{q_c}{q_{co}} = \frac{1+\sqrt{1+4CJa}}{2} \tag{2}$$

Where Ja is the Jacob number defined by Eq. (3) and C is given by Eq. (4).

$$Ja = \frac{c_p \Delta T_{sub}}{h_{fg}} \frac{\rho_l}{\rho_v} \tag{3}$$

$$C = \frac{0.95(d/D)^2(1+d/D)^{0.364}}{(\rho_l/\rho_v)^{0.43}\left(2\sigma/\rho_l u_j^2 (D-d)\right)^{0.343}} \tag{4}$$

Using Eqs. (1)–(4), the critical heat flux for the conditions given in Fig. 7 is 15.8 MW/m^2. Here D is taken to be the diameter of the apparent contact region for the jet (10 mm) rather than the diameter of the heater. It is clear that the heat fluxes estimated for the regions with and without the sheet flow pattern in Fig. 7 (3.7 MW/m^2 and 8 MW/m^2) are smaller than the estimated critical heat flux but have the same order of magnitude. This finding is very important to understanding the phenomena since it indicates that the boiling mode during the first 200 s of Figs. 6 and 7 is not well described by pure film boiling but rather it is somewhere between film boiling and the critical heat flux point.

The fact that the heat fluxes are lower than the estimated critical heat flux can be explained if we understand transition boiling to represent rapid cycles of contact and separation of the liquid and solid. During periods of contact at high temperatures, the heat flux may correspond to or be greater than the critical heat flux value, but if averaged over a cycle of contact and separation, the effective heat flux is lower. At higher temperatures the heat flux during contact will be higher but also the separation period will be longer resulting in a smaller average heat flux.

4. Discussion and possible explanation for observed phenomena

One of the most interesting results in the present investigation is the appearance and disappearance of the sheet flow pattern as the solid cooled. A similar phenomenon with a thin sheet of liquid lifting from the surface was also reported by Piggott et al. [8] and Hall et al. [10]. As was suggested, such lifted sheet phenomena are most likely the result of rapid vapor generation near the point where the liquid film lifts from the surface. The sheet then breaks into droplets further downstream due to surface tension. It may be possible that the flow pattern was different at higher temperatures due to transition boiling in the stagnation zone that changed to continuous contact nucleation boiling and then single-phase convection as the surface cooled [10].

Another factor that may contribute to explaining why the sheet flow pattern was not observed at temperatures greater than 300 °C in the present experiment is related to the superheat limit for the fluid. For water at atmospheric pressure the homogeneous nucleation temperature has been estimated to be in the range from 260 °C to 312 °C [13]. The change in flow structure occurred for an initial solid temperature above 300 °C for copper in Fig. 2 and at a slightly lower temperature for brass. The change in sound and slope of the cooling curve also occurred for solid temperatures in the vicinity of the homogeneous nucleation temperature as shown in Fig. 6. In Fig. 7, the best-fit analytical solution gave a surface temperature of 255^{+10}_{-30} °C at the center and 270 ± 10 °C at $r = 5$ mm for $t = 180$ s. If we assume that direct solid–liquid contact sometimes occurs at these temperatures then the interface temperature between the liquid and the solid will be of the order of magnitude necessary for homogeneous nucleation. This could explain why an explosive pattern appeared in Fig. 2(h) but not in Fig. 2(f). At higher temperatures during the brief instants of contact, a combination of homogeneous and heterogeneous nucleation may have occurred. At lower temperatures, only heterogeneous nucleation boiling occurred, which was not violent enough to rupture the liquid sheet. For initial temperatures lower than 200 °C conditions had been met for the liquid to continuously wet the surface and for the front to move forward so the flow pattern was again different.

A further important issue raised by the present study is how to interpret the observed phenomena in relation to the Leidenfrost point from the classical boiling curve. The Leidenfrost point is alternatively defined in the literature as the minimum heat flux condition or the point at which surface wetting starts or the point above which wetting does not occur. In the present experiment, the point at which surface wetting starts across the surface is at about 250 s in Fig. 7, which is after the sheet pattern had finished. However, the heat flux just before this time was estimated to be 8.0 MW/m^2, which seems too high for film boiling [9] and is certainly not the minimum heat flux condition in the present experiment.

Another possible choice for the Leidenfrost point is the changing point for where the sheet flow structure first appeared at around 180 s in Fig. 7. There was a sudden increase in heat flux at this point, which suggests that it could mark the change from stable film to transition boiling. However, if this hypothesis is correct, then contrary to expectation, we have a situation where stable film boiling was noisy while transition boiling was quiet. Other researchers [2,8,14] have suggested that evidence for stable film boiling is that there is no obvious boiling sound. This seems logical since the boiling sound is probably the result of rapid nucleation boiling during brief instants of transient contact.

Therefore in the present experiment, either the Leidenfrost point does not have a clear meaning or the Leidenfrost point is at a higher temperature than the initial solid temperature of 350 °C. This certainly would be consistent with the results of Ishigai et al. [2] and Liu and Wang [9] who suggested Leidenfrost points at superheats as high as ΔT_{sat} = 800 K (slot jet, ΔT_{sub} = 35 K) and ΔT_{sat} = 700 K (circular jet, ΔT_{sub} = 45 K) respectively for impinging water jets. The important consequence of this conclusion is that the observed phenomena in the present experiment (Figs. 2(e–h), 3 and 5(A) and (B)) are then classified as transition boiling phenomena in terms of the classical boiling curve. In other words, for solid temperatures in the range from 250 °C to 350 °C the surface was subjected to repeating cycles of wet and dry and stable film boiling could not be confirmed. This is very interesting since the regularity and duration of the observed phenomena indicates that transition boiling does not always proceed in chaotic or erratic manner. In fact, if the Leidenfrost point is significantly higher than the initial temperature of 350 °C, then the present work has confirmed the existence of distinctly different, stable transition boiling phenomena for impinging jets.

5. Conclusions

From the present experimental investigation the following conclusions can be drawn.

1. Unexpected boiling phenomena were observed during quench cooling of a cylindrical block of metal using an impinging jet of water.
2. The observed flow phenomenon changed depending on the initial temperature of the solid.
3. The change in flow pattern was accompanied by a change in boiling sound.
4. In the vicinity of a solid temperature of 300 °C, two distinctly different flow patterns could be observed.
5. The liquid sheet flow pattern corresponded to a greater heat flux and thus a faster cooling rate of the solid.
6. For a certain set of conditions the jet flow was found to oscillate between the two flow patterns—one with a sheet and one without a sheet. The frequency of the oscillation suggested a thermal effect accompanied by a change in boiling mode rather than a hydrodynamic effect or a fluctuation due to turbulence.
7. The high temperature phenomena observed as shown in Figs. 3 and 4 can be classified as transition boiling phenomena.
8. The meaning of the Leidenfrost point is a little unclear in the context of quench cooling by impinging jets both in the literature and in the present experiment.

Acknowledgments

The authors would like to thank Assoc. Prof. Y. Mitsutake for his helpful advice and support in carrying out this experimental research. The help of Dr. J. Hammad also is acknowledged gratefully.

Appendix A. Analytical solution for a finite cylinder with a step change in the heat flux boundary condition

The governing equation for heat conduction is given in Eq. (A.1).

$$\frac{1}{a}\frac{\partial T}{\partial t} = \frac{1}{r}\frac{\partial}{\partial r}\left(r\frac{\partial T}{\partial r}\right) + \frac{\partial^2 T}{\partial z^2} \tag{A.1}$$

The boundary conditions are specified in Eqs. (A.2a)–(A.2e).

$$q = -\lambda\frac{\partial T}{\partial z} = q_0 \quad (z = 0,\ r < r_0,\ t < t^*) \tag{A.2a}$$

$$q = -\lambda\frac{\partial T}{\partial z} = q_0^* \quad (z = 0,\ r < r_0,\ t > t^*) \tag{A.2b}$$

$$q = -\lambda\frac{\partial T}{\partial z} = q_1 \quad (z = 0,\ r > r_0) \tag{A.2c}$$

$$\frac{\partial T}{\partial z} = 0 \quad (z = H) \tag{A.2d}$$

$$\frac{\partial T}{\partial r} = 0 \quad (r = R, 0) \tag{A.2e}$$

The initial condition is a uniform temperature distribution as given in Eq. (A.3)

$$T(r, z, 0) = T_0 \tag{A.3}$$

The analytical solution to the problem specified in Eqs. (A.1)–(A.3) was derived using Laplace and Hankel transforms. The temperature at any point within the solid (r, z) is given as a function of time, t, in Eqs. (A.4) and (A.5).

$$T(r, z, t) = T_0 + G(q_0, r, z, t) \quad (t < t^*) \tag{A.4}$$

$$T(r, z, t) = T_0 + G(q_0, r, z, t) - G(q_0, r, z, (t - t^*)) + G\left(q_0^*, r, z, (t - t^*)\right) \quad (t > t^*) \tag{A.5}$$

where the function G is defined in Eqs. (A.6a)–(A.6g).

$$G(q_0, r, z, t) = C_0(F_1 - F_2) + \sum_{j=1}^{\infty}\left(J_0\left(m_j\frac{r}{R}\right)C_j(F_3 - F_4)\right) \tag{A.6a}$$

$$C_0 = \frac{H\left((q_0 - q_1)r_0^2 + q_1R^2\right)}{\lambda R^2} \tag{A.6b}$$

$$C_j = \frac{2H(q_0 - q_1)r_0 J_1\left(m_j \frac{r_0}{R}\right)}{\lambda m_j J_0^2(m_j) R} \tag{A.6c}$$

$$F_1 = \frac{at}{H^2} + \frac{1}{2}\left(1 - \frac{z}{H}\right)^2 - \frac{1}{6} \tag{A.6d}$$

$$F_2 = \sum_{k=1}^{\infty}\left((-1)^k \frac{2\cos\left(k\pi(1 - z/H)\right)\mathrm{e}^{-(k\pi)^2 at/H^2}}{(k\pi)^2}\right) \tag{A.6e}$$

$$F_3 = \frac{R\cosh\left(m_j \frac{H}{R}\left(1 - \frac{z}{H}\right)\right)}{Hm_j \sinh\left(m_j \frac{H}{R}\right)} - \frac{R^2 \mathrm{e}^{-m_j^2 \frac{at}{R^2}}}{H^2 m_j^2} \tag{A.6f}$$

$$F_4 = \sum_{k=1}^{\infty}\left((-1)^k \frac{2R^2\cos\left(k\pi(1 - z/H)\right)\mathrm{e}^{-\left(m_j^2 + (k\pi R/H)^2\right)at/R^2}}{H^2\left(m_j^2 + (k\pi R/H)^2\right)}\right) \tag{A.6g}$$

In Eq. (A.6) m_j is the j th root of Eq. (A.7).

$$J_1(m_j) = 0 \tag{A.7}$$

References

[1] D.H. Wolf, F.P. Incropera, R. Viskanta, Jet impingement boiling, Adv. Heat Transfer 23 (1993) 1–132.

[2] S. Ishigai, S. Nakanishi, T. Ochi, Boiling heat transfer for a plate water jet impinging on a hot surface, in: Proceedings of the 6th International Heat Transfer Conference, 1978, pp. 445–450.

[3] H. Auracher, W. Marquardt, Experimental studies of boiling mechanisms in all boiling regimes under steady-state and transient conditions, Int. J. Therm. Sci. 41 (2002) 586–598.

[4] H. Robidou, H. Auracher, P. Gardin, M. Lebouche, Controlled cooling of a hot plate with a water jet, Exp. Therm. Fluid Sci. 26 (2002) 123–129.

[5] J. Hammad, Y. Mitsutake, M. Monde, Movement of maximum heat flux and wetting front during quenching of hot cylindrical block, Int. J. Therm. Sci. 43 (2004) 743–752.

[6] J. Hammad, M. Monde, Y. Mitsutake, Characteristics of heat transfer and wetting front during quenching by jet impingement, Therm. Sci. Eng. 12 (2004) 19–26.

[7] M. Monde, H. Arima, W. Liu, Y. Mitutake, J.A. Hammad, An analytical solution for two-dimensional inverse heat conduction problems using Laplace transform, Int. J. Heat Mass Transfer 46 (2003) 2135–2148.

[8] B.D.G. Piggott, E.P. White, R.B. Duffey, Wetting delay due to film and transition boiling on hot surfaces, Nucl. Eng. Des. 36 (1976) 169–181.

[9] Z. Liu, J. Wang, Study on film boiling heat transfer for water jet impinging on high temperature flat plate, Int. J. Heat Mass Transfer 44 (2001) 2475–2481.

[10] D.E. Hall, F.P. Incropera, R. Viskanta, Jet impingement boiling from a circular free-surface jet during quenching: Part 1—Single-phase jet, J. Heat Transfer 123 (2001) 901–910.

[11] N. Hatta, J. Kokado, K. Hanasaki, Numerical analysis of cooling characteristics for water bar, Trans. Iron Steel Inst. Jpn. 23 (1983) 555–564.

[12] J. Rivallin, S. Viannay, General principles of controlled water cooling for metallurgical on-line hot rolling processes: forced flow and sprayed surfaces with film boiling regime and rewetting phenomena, Int. J. Therm. Sci. 40 (2001) 263–272.

[13] R. Cole, Boiling nucleation, Adv. Heat Transfer 10 (1974) 85–166.

[14] S. Kumagai, S. Suzuki, Y. Sano, M. Kawazoe, Transient cooling of a hot metal slab by an impinging jet with boiling heat transfer, in: Proceedings of the ASME/JSME Thermal Engineering Conference, vol. 2, 1995, pp. 347–352.

[15] M. Monde, Critical heat flux in saturated forced convective boiling on a heated disk with an impinging jet, Waerme- und Stoffuebertragung 19 (1985) 205–209.